Linear Frequency-domain Equalization Techniques for Continuous Phase Modulation

S.Narkees Begam[1], S.Mahalakshmi[2], R.Sundaresan
Department of ECE
[1, 2, 3]Assistant Professor,RVSETGI, Dindigul

Abstract-*This paper investigates the performance of reduced state trellis-based inter symbol interference equalizers, which are based on the so-called Ungerboeck and Forney observation models. Although the two models are equivalent when an optimum equalizer is employed, their performances differ significantly when using reduced-complexity methods. It is demonstrated that practical equalizers operating on the Forney model outperform those operating on the Ungerboeck model for high signal-to-noise ratios (SNRs), while the situation is reversed for low SNR levels. A novel reduced-complexity equalization strategy that improves on previous Ungerboeck-based equalizers is proposed. Alternatively, symbol rate MLSE with Ungerboeck formulation for classical DSSS radios was obtained. The complexity reduction technique based on reduced state sequence estimation (RSSE) with decision feedback is among the most common variations of the MLSE. A Forney type RSSE at symbol rate was studied for CCK modulation. Forney type reduced state algorithms are efficient and frequently employed with pre-filtering at reasonable complexity in practical applications such as Enhanced Data rates for Global System for Mobile Communications Evolution (GSM / EDGE) if the channel dispersion is limited with a moderate number of taps. Also, reduced state maximum a posteriori (MAP) detection was proposed to produce soft outputs based on Forney model in. ith the use of RSSE, the equivalence between Forney and Ungerboeck type structures begins to disappear, and Ungerboeck model may show certain advantages for channels with large delay spread.*

Keywords-Continuous phase modulation, equalizers, Global System for Mobile Communications Evolution (GSM / EDGE), Ungerboeck type & maximum a posteriori (MAP) telemetry.

I. INTRODUCTION

GENERAL modulation format is considered in this paper for linear channels impaired by additive white Gaussian noise (AWGN). This modulation can be represented as selection of one out of M waveforms per signaling interval to which an additional phase modulation is applied. We call this general type of signaling scheme M−ary quasi orthogonal signaling (MOS). Many modulation schemes such as M−ary orthogonal signaling for direct sequence spread spectrum (DSSS) radio in [1], [2], direct sequence code division multiple access (DS-CDMA) complementary code keying (CCK, M−ary bi-orthogonal keying (M-BOK) for ultra wideband (UWB) radio, and underwater acoustic (UWA) communication, standard phase shift keying (PSK); and recently proposed space shift keying (SSK) exploiting orthogonality in spatial domain can be put into this framework. This technique allows transmission with a low probability of interception, and simultaneous use of a common channel by multiple users. It is also suitable in military applications for combating jamming and self-interference. Due to the extremely high signal bandwidth of practical MOS waveforms, the multi-paths of the channel can be finely resolved at the receiver, which usually utilizes a RAKE processor to capture as much multi-path power as possible. However, the dense multi-path dispersion together with non−ideal correlation properties of the signaling waveforms may cause significant amount of inter-symbol interference (ISI), which necessitates equalizatio. In order to mitigate the effect of ISI, RAKE type correlators followed by chip rate unidirectional or bidirectional decision feedback (BDF)were investigated in without any regard to noise correlations at the RAKE outputs. There are also studies based on minimum mean squared error (MMSE) equalization at chip rate for DS-CDMA systems. Recently, conventional RAKE correlators were replaced by channel matched filter (CMF) to capture all the available multipath diversity. CMF followed by symbol rate decision feedback was proposed for M-BOK and CCK modulation. Our focus is on the maximum likelihood sequence estimation (MLSE) based equalization for the general modulation format MOS in this paper. MLSE-based receivers, which are optimal in the sense of lowest packet error rate, are based on one of the two classical approaches provided by Forney and Ungerboeck, which are known to be mathematically equivalent yet with rather different implementations.

II. PROPOSED SYSTEM

Optimum Maximum Likelihood Detection

The optimal detection rule based on MLSE finds the candidate sequence {IN,ΘN} of information symbols that

maximizes the likelihood of the received signal during one block duration, namely, r(t), $0 \le t \le T0$ in terms of MF outputs and waveform correlations. The optimal detector is composed of a CMF followed by M code matched filters corresponding to different signaling waveforms gi(t) and MLSE type processing operating at symbol rate. The first term corresponds to the MF operation and the last term is related to the cancellation of ISI and multi code interference (MCI) which is the cross interference among MF outputs caused by the channel and thenon−ideal correlation properties of the signaling waveforms

Project description

This paper investigates the performance of reduced state trellis-based inter symbol interference equalizers, which are based on the so-called Ungerboeck and Forney observation models. Although the two models are equivalent when an optimum equalizer is employed, their performances differ significantly when using reduced-complexity methods. It is demonstrated that practical equalizers operating on the Forney model outperform those operating on the Ungerboeck model for high signal-to-noise ratios (SNRs), while the situation is reversed for low SNR levels. A novel reduced-complexity equalization strategy that improves on previous Ungerboeck-based equalizers is proposed

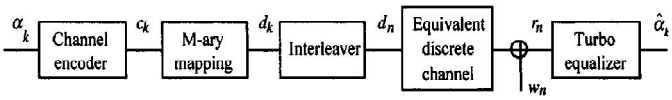

Principle of the transmission scheme.

Decomposition of MLSE We have described how the VA can be truncated such that the memory requirement is significantly reduced with little loss in performance. Define a k-dimensional MLSE as one with truncation depth k. Then a TVA with truncation depth δ can be viewed as a way to implement a δ-dimensional MLSE, in which the path metrics are initialized according to the calculation of the previous MLSE.

In general, if the performance is dominated by the minimum distance error events, the effect of truncation should be negligible independent of the way to implement the δ-dimensional MLSE. Based on this argument, we introduce a "natural" way to decompose a l-dimensional MLSE into l δ-dimensional MLSE's. Let us consider a l-dimensional MLSE which finds the detected sequence ˆx = (ˆxl, ˆxl−1, · · ·, ˆx1) from the received sequence z = (zl+v, zl+v−1, · · ·, z1). If the truncation depth δ is chosen such that it satisfies proposition 2.1, most survivor paths with small path metric at stage δ will merge together at the first stage and all symbols associated with the merged path can be decided. Thus assuming that all survivor paths originated from a single known node associated with the previous decisions should cause little loss in performance. Let the feedback sequence (ˆxi−1, ˆxi−2, · · · , ˆxi−v) be the v detected symbols before xi. To estimate xi, we only need a δ-dimensional MLSE to find a detected sequence (˜xi+δ−1, ˜xi+δ−2, · · · , ˜xi) from the received sequence (zi+δ−1, zi+δ−2, · · · , zi) with decision feedback from (ˆxi−1, ˆxi−2, · · ·, ˆxi−v). Then thesymbol ˜xi estimated is released as the detected symbol ˆxi. To estimate the next symbol xi+1, the estimator then find the detected sequence (˜xi+δ, ˜xi+δ−1, · · · , ˜xi+1) from the received sequence (zi+δ, zi+δ−1, · · ·, zi+1) with the new feedback sequence (ˆxi, ˆxi−1, · · · , ˆxi−v+1). The symbol ˜xi+1 estimated is released as the detected symbol ˆxi+1. In this way, the detected symbol sequence is found symbol by symbol. We say that the estimator is operating in an incremental mode. As a result, we can apply a single δ-dimensional MLSE to detect a sequence of l symbols in l passes.

Sum-product algorithm

The sum-product algorithm is the basic "decoding" algorithm for codes on graphs. For finite cycle-free graphs, it is finite and exact. However, because all its operations are local, it may also be applied to graphs with cycles; then it becomes iterative and approximate, but in cod¬ing applications it often works very well. It has become the standard decoding algorithm for capacity-approaching codes (e.g., turbo codes, LDPC codes).

There are many variants and applications of the sum-product algorithm. The most straight¬forward application is to a posteriori probability (APP) decoding. When applied to a trellis, it becomes the celebrated BCJR decoding algorithm. In the field of statistical inference, it becomes the even more widely known "belief propagation" (BP) algorithm. For Gaussian state-space models, it becomes the Kalman smoother.

There is also a "min-sum" or maximum-likelihood sequence detection (MLSD) version of the sum-product algorithm. When applied to a trellis, the min-sum algorithm gives the same result as the Viterbi algorithm.

Reduced State Sequence Estimation (RSSE)

The strong impact of ISI due to multipath propagation or narrow bandwidth (e.g., 2G-GSM bandwidth is narrower than corresponding symbol rate) can cause severe signal distortion, which requires sophisticated equalization approaches. Maximum likelihood sequence estimation

(MLSE), based on the Viterbi algorithm, is the optimum solution for channel equalization and signal detection. Unfortunately, the computational complexity of MLSE grows exponentially with the number of bits per symbol and with the delay spread of the multipath channel. The combination of a high modulation order and long channels renders MLSE infeasible in modern wireless systems. A sub-optimal Viterbi equalizer that can achieve close-to-MLSE performance1 at significantly lower complexity is reduced-state sequence estimation (RSSE). Contrary to MLSE where reference signals that correspond to all possible combinations of modulated symbol sequences with channel length L are compared with the received signal, RSSE drastically reduces the number of candidate symbol sequences by applying symbol partitioning and decision feedback with early decisions (cf. Sec. 2). Since the generation of the reference signals is the most complex part of MLSE, the reduction of candidate symbol sequences with RSSE directly translates to a reduction of corresponding implementation complexity. Unfortunately, even RSSE complexity is still huge when supporting high modulation orders. Hence, dedicated hardware is required to achieve high throughput or to achieve hardware and energy efficient solutions, as desired for mobile devices. Compared to MLSE, the RSSE algorithm reduces the number of trellis states by dividing the symbol alphabet into subsets and defining the trellis on these subsets. The division of the M symbols into J subsets is optimally chosen such that the Euclidean distance of symbols within the same subset is maximal (e.g., through Ungerboeck partitioning). Whenever a surviving path is selected, a decision within the subset is done immediately, but the selection among subsets is postponed.

III. RSSE IMPLEMENTATION FOR EVOLVED EDGE

In order to show the suitability of our design-space exploration for VLSI implementation, we have implemented an RSSE solution for a 2.75G E-EDGE baseband transceiver in dedicated hardware. Tothis end, the implemented RSSE supports GMSK, 8PSK, 16QAM and 32QAM modulation, and processes 2 trellises of 58 symbols per GSM burst (cf.,) For 16QAM and 32QAM, the RSSE is configured (4=2=2) with 16 trellis states, and for 8PSK and GMSK modulation the RSSE is configured (2=2=2) with 8 states. Simulations have shown that these RSSE configurations provide close-to-MLSE performance for the different modulation types when applying a channel shortening filter in front of the RSSE. As storage requirements for a 16-state trellis are fairly low, the combined pre-computation approach was chosen and the es of all16 predecessor states and the eb of all 32 possible symbols are precomputed (cf. Sec. 3). Thus, the number of multiplications per trellis stage has been greatly reduced from 4096 (no pre-computation) to 144 at the cost of a storage capacity of 48 pre-computed words. Modern wireless communication receivers require high-performance channel equalizer solutions that meet the (moderate) throughput requirement sat reasonably low complexity. RSSE is a suitable candidate that allows for a multitude of algorithmic and architectural realizations. To this end, the concept of pre-computation enables a significant reduction of computational complexity at the cost of a small amount of storage capacity in RSSE implementations. The efficiency of RSSE architectures with pre-computation has been shown with our measured ASIC implementation of a 2.75G channel equalizer, that achieves a 1.6 times higher hardware efficiency, when compared to a corresponding DDFSE design with similar performance.

Channel matched filter

The matched filter is the optimal linear filter for maximizing the signal to noise ratio (SNR) in the presence of additive stochastic noise. Matched filters are commonly used in radar, in which a signal is sent out, and we measure the reflected signals, looking for something similar to what was sent out.

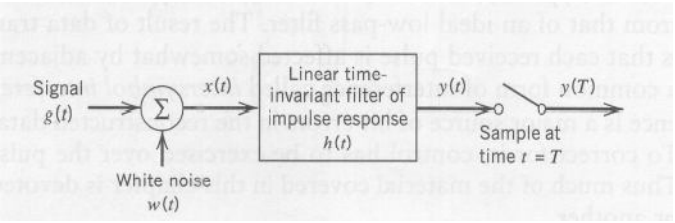

GPD is widely used in fields of finance, meteorology, material engineering, etc… to for the prediction of extreme or rare events which are normally known as the exceedances. However, GPD has not yet been applied in optical communications to obtain the BER. The following reasons suggest that GPD may become a potential and a quick method for evaluation of an optical system, especially when non-linearity is the dominant degrading factor to the system performance.

1. The normal distribution has a fast roll-off, i.e. short tail. Thus, it is not a good fit to a set of data involving exeedances, i.e. rarely happening data located in the tails of the distribution. With a certain threshold value, the generalized Pareto distribution can be used to provide a good fit to extremes of this complicated data set.
2. When nonlinearity is the dominating impairment degrading the performance of an optical system, the sampled received signals usually introduce a long tail distribution. For example, in case of DPSK optical system, the distribution of nonlinearity phase noise differs

from the Gaussian counterpart due to its slow roll-off of the tail. As the result the conventional BER obtained from assumption of Gaussian-based noise is no longer valid and it often underestimates the BER.

3. A wide range of analytical techniques have recently been studied and suggested such as importance sampling, multi-canonical method, etc. Although these techniques provide solutions to obtain a precise BER, they are usually far complicated. Whereas, calculation of GPD has become a standard and available in the recent Matlab version (since Matlab 7.1). GPD therefore may provide a very quick and convenient solution for monitoring and evaluating the system performance. Necessary preliminary steps which are fast in implementation need to be carried out the find the proper threshold.
4. Evaluation of contemporary optical systems requires BER as low as 1e-15. Therefore, GPD can be seen quite suitable for optical communications.

Selection of Threshold for GPD Fitting

Using this statistical method, the accuracy of the obtained BER strongly depend on the threshold value (Vthres) used in the GPD fitting algorithm, i.e. the decision where the tail of the GPD curve starts.

There have been several suggested techniques as the guidelines aiding the decision of the threshold value for the GPD fitting. However, they are not absolute techniques and are quite complicated. In this paper, a simple technique to determine the threshold value is proposed. The technique is based on the observation that the GPD tail with exceedances normally obeying a slow exponential distribution compared to the faster decaying slope of the distribution close to the peak values. The inflection region between these two slopes gives a good estimation of the threshold value for GPD fitting. This is demonstrated in Figure 13.

Whether the selection of the Vthres value leads to an adequately accurate BER or not is evaluated by using the cumulative density function (cdf-Figure 14) and the quantile-quantile plot (QQ plotFigure 15). If there is a high correlation between the pdf of the tail of the original data set (with a particular Vthres) and pdf of the GPD, there would be a good fit between empirical cdf of the data set with the GPD-estimated cdf with focus at the most right region of the two curves. In the case of the QQ-plot, a linear trend would be observed. These guidelines are illustrated in Figure 14. In this particular case, the value of 0.163 is selected to be Vthres.

Furthermore, as a demonstration of improper selection of Vthres, the value of 0.2 is selected.Figure 16 and Figure 17 show the non-compliance of the fitted curve with the GPD which is reflected via the discrepancy in the two cdfs and the nonlinear trend of the QQ-plot.

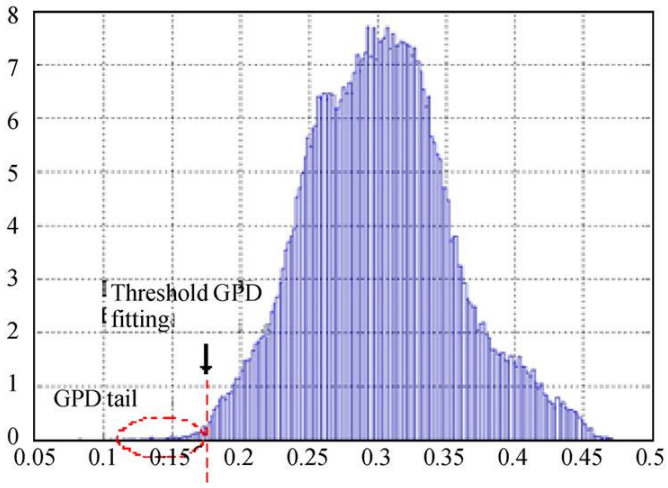

Selection of threshold for GPD fitting.

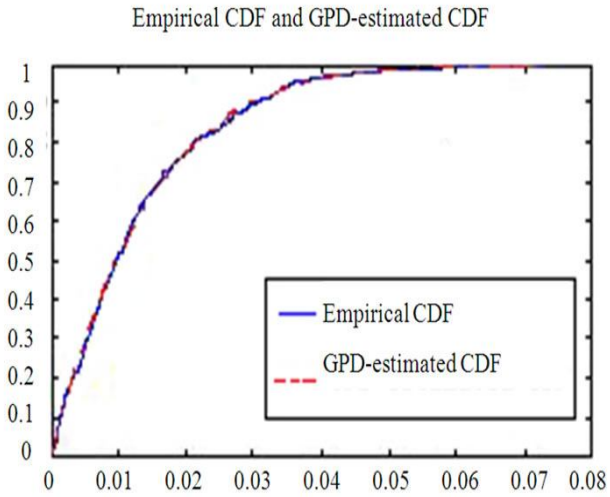

Comparison between fitted and empirical cumulative distribution functions.

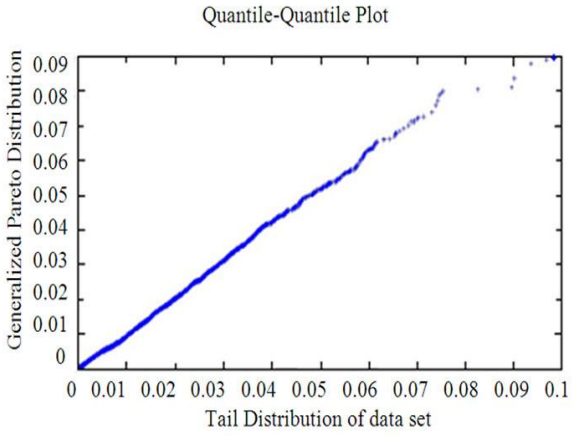

Quantile-quantile plot.

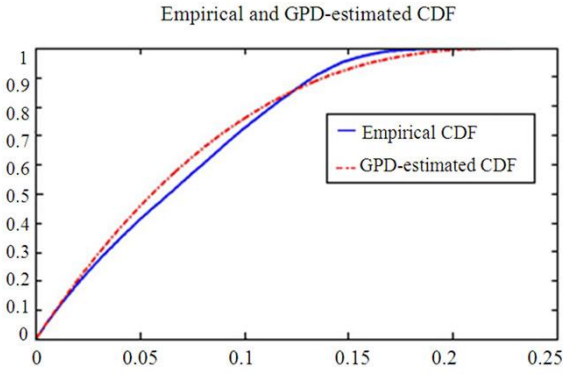

Comparison between fitted and empirical cumulative distribution functions.

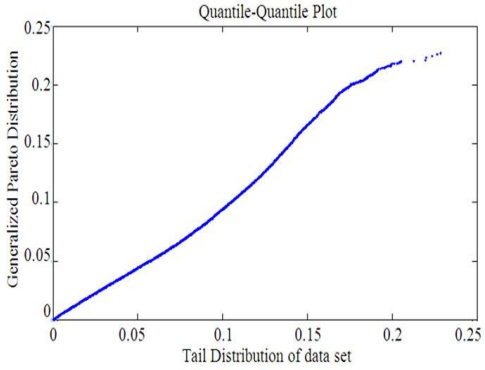

Quantile-quantile plot.

Validation of the Statistical Methods

A simulation test-bed of an optical DPSK transmission system over 880 km SSMF dispersion managed optical link (8 spans) is set up. Each span consists of 100 km SSMF and 10 km of DCF whose dispersion values are +17 ps/nm.km and -170 ps/nm.km at 1550 nm wavelength respectively and fully compensated i.e zero residual dispersion. The average optical input power into each span is set to be higher than the nonlinear threshold of the optical fiber. The degradation of the system performance hence is dominated by the nonlinear effects which are of much interest since it is a random process creating indeterminate errors in the long tail region of the pdf of the received electrical signals.

The BER results obtained from the novel statistical methods are compared to that from the Monte-Carlo simulation as well as from the semi-analytical method. Here, the well-known analytical expression to obtain the BER of the optical DPSK format is used, given as [30].

$$BER = \frac{1}{2} - \frac{\rho e^{-\rho}}{2} \sum_{k=0}^{\infty} \frac{(-1)^k}{2k+1} \left[I_k\left(\frac{\rho}{2}\right) + I_{k+1}\left(\frac{\rho}{2}\right) \right]^2 e^{-\frac{1}{2}(2k+1)^2 \sigma_{NLP}^2}$$

where ρ is the obtained OSNR and σ_{NLP}^2 is the variance of nonlinear phase noise.

In this case, in order to calculate the BER of a optical DPSK system involving the effect of nonlinear phase noise, the required parameters including the OSNR and the variance of nonlinear phase noise etc are obtained from the simulation numerical data which is stored and processed in Matlab. The fitting curves implemented with the MGD method for the pdf of bit 0 and bit 1 (input power of 10 dBm) as shown in Figure 18 and illustrated in Figure 19 for bit 0 and bit 1 respectively.

The selection of optimal threshold for GPD fitting follows the guideline as addressed in detail in the previous section. The BER from various evaluation methods are shown in Table 1. The input powers are controlled to be 10 dBm and 11 dBm.

Table 1 validates the adequate accuracy of the proposed novel statistical methods with the discrepancies compared to the Monte-Carlo and semi-analytical BER to be within one decade. In short, these methods offer a great deal of fast processing while maintaining the accuracy of the obtained BER within the acceptable limits.

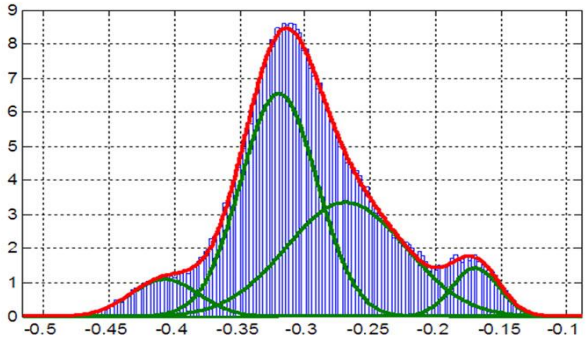

Demonstration of fitting curves for bit ‘0’ with MGD method.

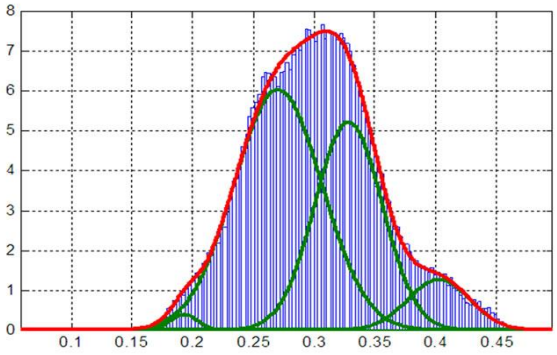

Demonstration of fitting curves for bit ‘0’ with MGD method.

Input Power \ Evaluation Methods	Monte-Carlo Method	Semi-analytical Method	MGD method	GPD method
10 dBm	1.7e-5	2.58e-5	5.3e-6	3.56e-4
11 dBm		1.7e-8	2.58e-9	4.28e-8

Table 1. The BER from various evaluation methods.

Summary

We have demonstrated the Simulink modeling of amplitude and phase modulation formats at 40 Gb/s optical fiber transmission. A novel modified fiber propagation algorithm has been used to minimize the simulation processing time and optimize its accuracy. The principles of amplitude and phase modulation, encoding and photonic-opto-electronic balanced detection and receiving modules have been demonstrated via Simulink modules and can be corroborated with experimental receiver sensitivities.

The XPM and other fiber nonlinearity such as the Raman scattering, four wave mixing are not integrated in the Matlab Simulink models. A switching scheme between the linear only and the linear and nonlinear models is developed to enhance the computing aspects of the transmission model.

Other modulations formats such as multi-level MDPSK, M-ASK that offer narrower effective bandwidth, simple optical receiver structures and no chirping effects would also be integrated. These systems will be reported in future works. The effects of the optical filtering components in DWDM transmission systems to demonstrate the effectiveness of the DPSK and DQPSK formats, have been measured in this paper and will be verified with simulation results in future publications. Finally, further development stages of the simulator together with simulation results will be reported in future works.

IV. CONCLUSION

We have illustrated the modeling of various schemes of advanced modulation formats for optical transmission systems. Transmitter modules integrating lightwaves sources, electrical pre-coder and external modulators can be modeled without difficulty under MATLAB Simulink. As the popularity of MATLAB becoming a standard computing language for academic research institutions throughout the world, the models reported here would contribute to the wealth of computing tools for modeling optical fiber transmission systems and teaching undergraduates at senior level and postgraduate research scholars. The models can integrate photonic filters or other photonic components using blocksets available in Simulink. Furthermore we have used the developed models to assess the effectiveness of the models by evaluating the simulated results and experimental transmission performance of long haul advanced modulation format transmission systems.

REFERENCES

[1] L. N. Binh, “Tutorial Part I on optical systems design,” ECE 4405, ECSE Monash University, Australia, presented at ICOCN 2002.
[2] T. Kawanishi, S. Shinada, T. Sakamoto, S. Oikawa, K. Yoshiara, and M. Izutsu, “Reciprocating optical modulator with resonant modulating electrode,” Electronics Letters, Vol. 41, No. 5, pp. 271-272, 2005.
[3] R. Krahenbuhl, J. H. Cole, R. P. Moeller, and M. M. Howerton, “High-speed optical modulator in LiNbO3 with cascaded resonant-type electrodes,” Journal of Lightwave Technology, Vol. 24, No. 5, pp. 2184-2189, 2006.
[4] I. P. Kaminow and T. Li, “Optical fiber communications,” Vol. IVA, Elsevier Science, Chapter 16, 2002.
[5] G. P. Agrawal, “Fiber-optic communications systems,” 3rd edition, John Wiley & Sons, 2001.
[6] J. B. Jeunhomme, “Single mode fiber optics,” Principles and Applications, 2nd edition: Marcel Dekker Pub, 1990.
[7] E. E. Basch, (Editor in Chief), “Optical-fiber transmission,” 1st edition, SAMS, 1987.
[8] I. P. Kaminow and T. Li, “Optical fiber communications,” Vol. IVB, Elsevier Science (USA), Chapter 5, 2002.
[9] J. P. Gordon and H. Kogelnik, “PMD fundamentals: Polarization mode dispersion in optical fibers,” PNAS, Vol. 97, No. 9, pp. 4541-4550, April 2000.
[10] Corning. Inc, “An introduction to the fundamentals of PMD in fibers,” White Paper, July 2006.
[11] A. Galtarossa and L. Palmieri, “Relationship between pulse broadening due to polarisation mode dispersion and differential group delay in long singlemode fiber,” Electronics Letters, Vol. 34, No. 5, March 1998.
[12] J. M. Fini and H. A. Haus, “Accumulation of polarization-mode dispersion in cascades of compensated optical fibers,” IEEE Photonics Technology Letters, Vol. 13, No. 2, pp. 124-126, February 2001.
[13] A. Carena, V. Curri, R. Gaudino, P. Poggiolini, and S. Benedetto, “A time-domain optical transmission system simulation package accounting for nonlinear and polarization-related effects in fiber,” IEEE Journal on Selected Areas in Communications, Vol. 15, No. 4, pp. 751-765, 1997.
[14] S. A. Jacobs, J. J. Refi, and R. E. Fangmann, “Statistical estimation of PMD coefficients for system design,” Electronics Letters, Vol. 33, No. 7, pp. 619-621, March 1997.

[15] E. A. Elbers, International Journal Electronics and Communications (AEU) 55, pp 195-304, 2001.
[16] T. Mizuochi, K. Ishida, T. Kobayashi, J. Abe, K. Kinjo, K. Motoshima, and K. Kasahara, "A comparative study of DPSK and OOK WDM transmission over transoceanic distances and their performance degradations due to nonlinear phase noise," Journal of Lightwave Technology, Vol. 21, No. 9, pp. 1933-1943, 2003.
[17] H. Kim, "Differential phase shift keying for 10-Gb/s and 40-Gb/s systems," in Proceedings of Advanced Modulation Formats, 2004 IEEE/LEOS Workshop on, pp. 13-14, 2004.
[18] P. J. T. Tokle., "Advanced modulation fortmas in 40 Gbit/s optical communication systems with 80 km fiber spans," Elsevier Science, July 2003.
[19] Elbers, et al., International Journal of Electronics Communications (AEU) 55, pp 195-304, 2001.
[20] J. P. Gordon and L. F. Mollenauer, "Phase noise in photonic communications systems using linear amplifiers," Optics Letters, Vol. 15, No. 23, pp. 1351-1353, December 1990.
[21] G. Jacobsen, "Performance of DPSK and CPFSK systems with significant post-detection filtering," IEEE Journal of Lightwave Technology, Vol. 11, No. 10, pp. 1622-1631, 1993.
[22] A. F. Elrefaie and R. E. Wagner, "Chromatic dispersion limitations for FSK and DPSK systems with direct detec tion receivers," IEEE Photonics Technology Letters, Vol. 3, No. 1, pp. 71-73, 1991.
[23] A. F. Elrefaie, R. E. Wagner, D. A. Atlas, and A. D. Daut, "Chromatic dispersion limitation in coherent lightwave systems", IEEE Journal of Lightwave Technology, Vol. 6, No. 5, pp. 704-710, 1988.
[24] D. E. Johnson, J. R. Johnson, and a. H. P. Moore, "A handbook of active filters," Englewood Cliffs, New Jersey: Prentice-Hall, 1980.
[25] J. G. Proakis, "Digital communications," 4th edition, New York: McGraw-Hill, 2001.